A Large-Scale Multi-Column Spiking Network Model of the Prefrontal Cortex

Pedro R. Pinheiro[1], Renan O. Shimoura[2], Arthur R. Rodrigues[3], Rafael F. Gigante[1], Markus Diesmann[2,4,5,6], Sacha J. van Albada[2,7], Antonio C. Roque[1]

[1] Physics Department, University of São Paulo, Brazil
[2] Institute for Advanced Simulation (IAS-6), Jülich Research Centre, Germany
[3] Department of Electrical Engineering, Federal University of Minas Gerais, Brazil
[4] JARA-Institute Brain Structure-Function Relationships (INM-10), Jülich Research Centre, Germany
[5] Department of Psychiatry, Psychotherapy and Psychosomatics, RWTH Aachen University, Germany
[6] Department of Physics, RWTH Aachen University, Germany
[7] Institute of Zoology, University of Cologne, Germany

Contact: ribeirop406@gmail.com

Introduction

Despite the central role of the prefrontal cortex (PFC) in higher cognitive function, many aspects of its large-scale dynamics remain poorly understood. Here, we present a data-driven, biologically constrained spiking neural network model of the human PFC implemented with the NEST simulator[1]. Building upon the network first described in [2], our approach employs adaptive exponential integrate-and-fire (AdEx) neurons[3] in a large-scale multi-column network architecture and incorporates an external thalamic population.

Methods

Network anatomy

- Over 60,000 neurons and around 1 billion synapses, with realistic neuron and synapse densities adopted from the human rostral anterior cingulate area[4].

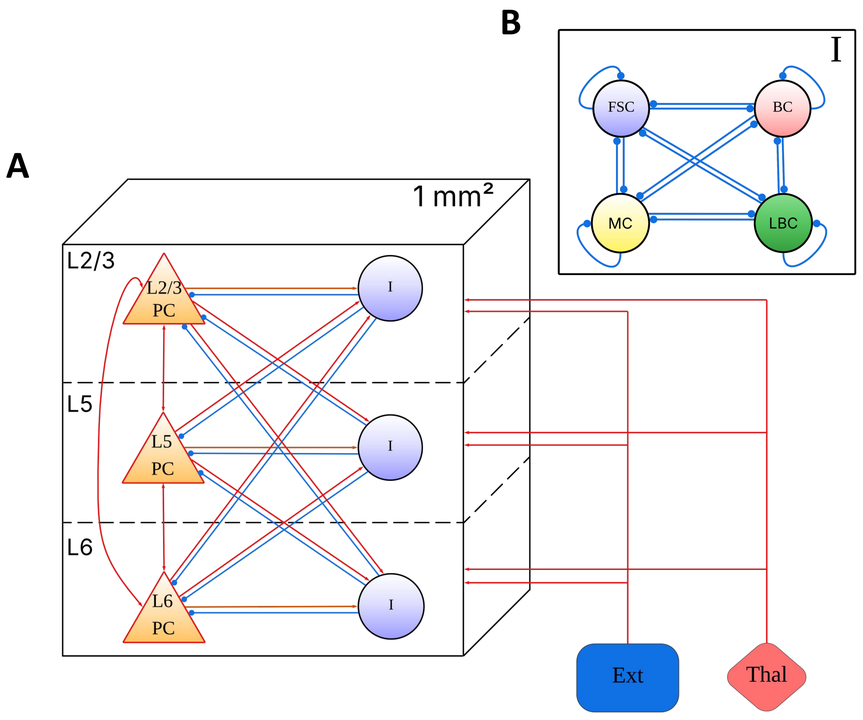


Fig. 1: Network anatomy. A: Laminar structure of the network. L2/3: Layer 2/3, L5: Layer 5, L6: Layer 6. PC: Pyramidal cell, I: Inhibitory cell types (see B). Ext: External input. Thal: Thalamic population. Excitatory connections depicted in red and inhibitory connections in blue. **B:** Four different inhibitory cell types are present in the model. FSC: Fast-spiking cells, BC: Bitufted cells, MC: Martinotti cells, LBC: Large basket cells.

Neuron model and biophysics

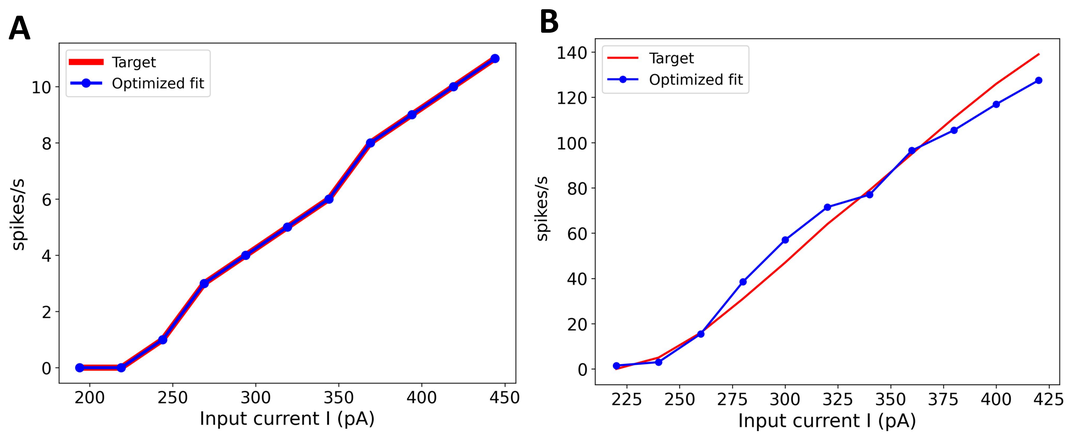
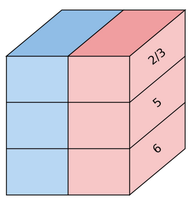


Fig. 2: Parameter optimization. AdEx model parameters of individual cell types were optimized to fit experimental f-I curves, spike train behavior and biophysical properties using an evolutionary algorithm (scipy.optimize.differential_evolution). Representative f-I curve fitting traces are depicted for L2/3 PCs (**A)** and FSCs (**B**).

- AMPA, $GABA_a$ and NMDA synapses.
- Advanced STP rules defined following a revised Tsodyks-Markram formulation[5].
- Most of the plasticity parameters, connection probabilities and synaptic conductances and weights were adapted from [2]. L6 shares most of its synaptic parameters with L5, with reduced connection probabilities between both layers.

Joint E/I clustering

- 50 columns (Q) under 1 mm^2 of surface area defined using the joint E/I clustering algorithm described in [6].



$$J_{I+} = 1 + R_J(J_{E+} - 1) \qquad J_{E-} = \frac{Q - J_{E+}}{Q - 1} \qquad J_{I-} = \frac{Q - J_{I+}}{Q - 1}$$

Fig. 3: Clustering rule. Inside the clusters, synaptic weights are strengthened by factors J_{E+}(excitatory) and J_{I+}(inhibitory). Between clusters, weights are reduced by the respective factors J_{E-} and J_{I-}. R_J is a proportionality factor of 0.75.

Thalamic input

- 902 parrot neurons firing at 2Hz implemented using an adapted version of the thalamic population in [7].
- Mediodorsal thalamic properties, with stronger input to L2/3[8].

External input

- Poisson spike trains with a rate defined by the number of synapses arriving from outside the simulated column[2]. Cell-type specific scaling was applied to the synaptic weights.

Results

Clustering weight factor (J_{E+}) dictates transitions between firing states

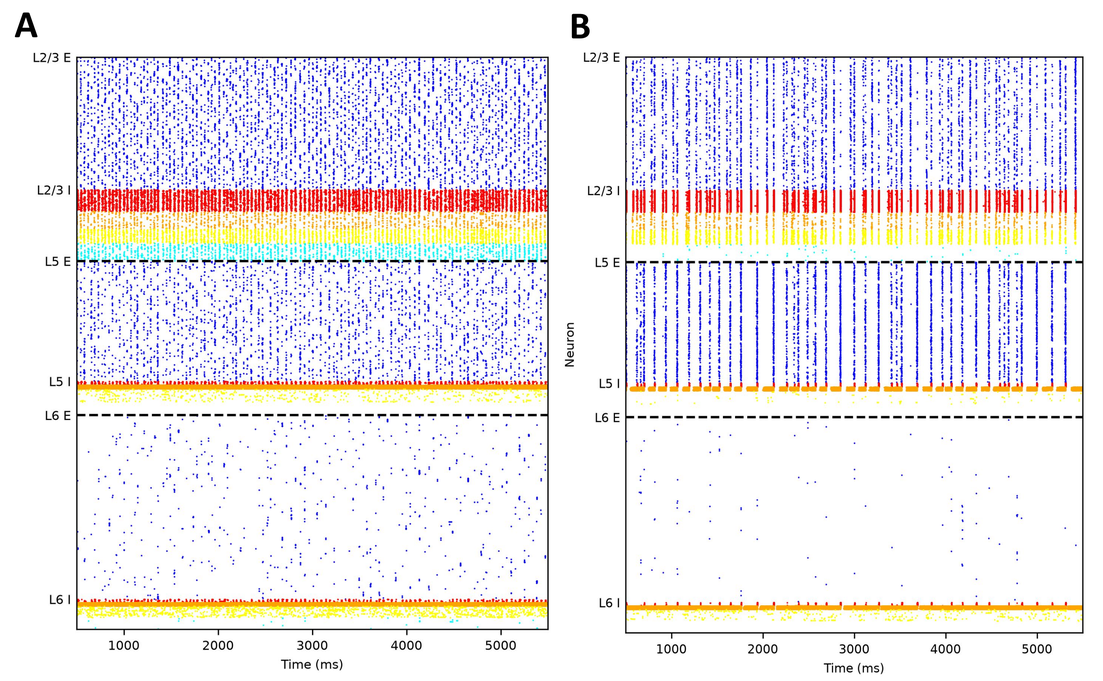


Fig. 4: Raster plots depicting the dynamics of distinct firing states. Blue: PCs, red: FSCs, orange: BCs, yellow: MCs, cyan: LBCs. Regularity was measured using the CV2 metric[9] and synchrony using the Spike Time Tilling Coefficient (STTC)[10]. **A: J_{ex} = 25.** Asynchronous Irregular (AI) state (CV2 = 0.92; STTC = 0.008). Pyramidal cells exhibit sparse spontaneous firing, consistent with low firing rates reported in awake PFC.[11] **B: J_{ex} = 8.** Synchronous Irregular state (CV2 = 0.89; STTC = 0.028).

Preliminary spectral validation

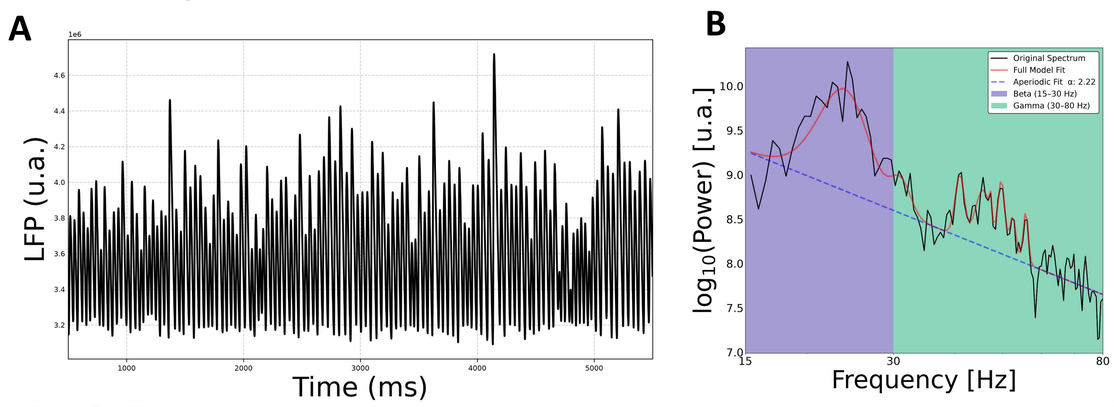


Fig. 5: The network exhibits spontaneous activity at the beta and gamma ranges and a realistic aperiodic exponent while in the AI state. A: LFP proxy signal estimated by the sum of the absolute values of all synaptic currents for every time point, as described in [12]. **B:** Power spectral density of the LFP signal obtained using the Welch method. The "fixed" mode of the FOOOF tool[13] was employed in order to detect oscillatory peaks and fit the aperiodic exponent of 2.22. An exponent close to 2 for frequencies below 80 Hz was reported previously in an experiment with human subjects[14].

Summary

- We developed a data-driven full-scale multi-column PFC network in NEST.
- The clustering weight factor J_{E+} plays a key role in network synchrony.
- In the AI state, the network exhibits spontaneous oscillatory activity and an aperiodic exponent similar to one obtained experimentally.
- Overall, the model provides a flexible platform for investigating how laminar structure, synaptic physiology, and thalamocortical interactions shape large-scale PFC dynamics across different activity states in mammalian cortical systems.

References

1. Gewaltig, M.-O. and Diesmann, M. NEST (NEural Simulation Tool), Scholarpedia J.2(4): 1430. 2007.
2. Hass, J., Hertäg, L. and Durstewitz, D. A detailed data-driven network model of prefrontal cortex reproduces key features of in vivo activity, PLoS Comput. Biol. 12(5): e1004930. 2016.
3. Brette, R.; Gerstner, W. Adaptive exponential integrate-and-fire model as an effective description of neuronal activity. Journal of Neurophysiology, v. 94, p. 3637–3642, 2005.
4. Pronold, J. et al. Multi-scale spiking network model of human cerebral cortex. Cerebral Cortex, Oxford University Press, v. 34, 10 2024.
5. Maass W, and Markram H. Synapses as dynamic memory buffers. Neural Netw. 15:155–161, 2002.
6. Rostami, V., Rost, T., Schmitt, F. J., van Albada, S. J., Riehle, A., & Nawrot, M. P. Spiking attractor model of motor cortex explains modulation of neural and behavioral variability by prior target information. *Nature Communications*, *15*(1), 6304. 2024.
7. Potjans, T. C., Diesmann, M. The cell-type specific cortical microcircuit: relating structure and activity in a full-scale spiking network model. Cerebral Cortex, v. 24, p. 785–806, 2014.
8. Collins D. P., Anastasiades P. G., Marlin J. J., Carter A. G. . Reciprocal Circuits Linking the Prefrontal Cortex with Dorsal and Ventral Thalamic Nuclei. Neuron. 2018.
9. Holt G. R., Softky W. R., Koch C., Douglas R. J. . Comparison of discharge variability in vitro and in vivo in cat visual cortex neurons. J Neurophysiol. 1996.
10. Cutts C. S., Eglen S. J. . Detecting pairwise correlations in spike trains: an objective comparison of methods and application to the study of retinal waves. J Neurosci. 2014.
11. Boudewijns, Z. S., Groen, M. R., Lodder, B., McMaster, M. T., Kalogreades, L., de Haan, R., Narayanan, R. T., Meredith, R. M., Mansvelder, H. D., & de Kock, C. P. Layer-specific high-frequency action potential spiking in the prefrontal cortex of awake rats. Frontiers in cellular neuroscience, 7, 99. 2013.
12. Mazzoni, A. et al. Computing the local field potential (lfp) from integrate-and-fire network models. PLoS computational biology, v. 11, p. e1004584, 12 2015.
13. Donoghue, T., Haller, M., Peterson, E.J. *et al.* Parameterizing neural power spectra into periodic and aperiodic components. Nat Neurosci. 2020.
14. Miller, K. J., Sorensen, L. B., Ojemann, J. G. and den Nijs, M. Power-law scaling in the brain surface electric potential, PLoS Comput. Biol. 5(12): e1000609. 2009.

Member of the Helmholtz Association

Acknowledgements: This work was supported by FAPESP (scholarships 2024/16557-9 and 2026/02588-5 to PRP and 2025/19941-7 to RFG), FAPEMIG (grant 14216 to ARR), CNPq (INCT-NeuroComp grant 408389/2024-9 and productivity research grant 303359/2022-6 to ACR) and the Horizon Europe Grant 101147319. The opinions, hypotheses, and conclusions or recommendations expressed herein are those of the authors and do not necessarily reflect the views of FAPESP, FAPEMIG, or CNPq.